Technical University of Varna Annual Journal
https://doi.org/10.29114/ajtuv.vol8.iss1.303
Vol. 8 Issue 1 (2024)
Published: 2024-06-28
ISSN 2603-316X (Online)

Elastic constants of iron base sintered alloys after chemical heat treatment

Desislava Mincheva[1], *Plamen* Petrov[1], and *Diyan* Dimitrov[2]

1 – Technical University of Varna, Department of Materials Science and Technology, 9010, 1 Studentska Street, Varna, Bulgaria
2 – Technical University of Varna, Department of Mechanics and Machine Elements, 9010, 1 Studentska Street, Varna, Bulgaria

Corresponding author contact: mincheva_d@abv.bg

Abstract. In this paper is shown the effect of applied low-temperature gas nitrocarburizing on the elastic constants and mechanical properties of iron based sintered alloys. Low temperature gas nitrocarburizing (LTGNC) was carried out under laboratory conditions at T=550°C, and short saturation times of 15 and 30 min, respectively. The process was carried out in a laboratory shaft furnace with a volume of 2 dm^3, in ammonia and carbon dioxide at an HN_3/CO_2=7.5/1 ratio. The elastic constants were determined using a standard dynamic methodology based on a pulse resonance method. Density and porosity of the samples were determined. A metallographic analysis of the microstructure after sintering and after chemical heat treatment was carried out.

Keywords: sintered alloys, low temperature gas nitrocarburizing (LTGNC), impulse resonance method, elastic constants, Young's modulus, microstructures

1 Introduction

Sintered alloys based on iron or also known as powder-metallurgical materials (PM) are widely used in various branches of mechanical engineering. As the main user of this type of details can be pointed out the automotive industry. About 90% of the parts used in this sector are made precisely by conventional technologies of pressing and sintering of iron powders or mechanical mixtures. The reason for this is that through the technologies of powder metallurgy, details with a complex configuration can be made, possessing unique structure and properties. The main characteristic of sintered components is the porosity, which affects their elastic constants, mechanical properties etc. (German, 1994) (Chawla & Deng, 2005).

Chemical heat treatment, especially gas nitrocarburizing, is an affordable technology that is used to increase the mechanical properties of sintered alloys. The presence of pores in the structure promotes accelerated saturation of the metal base and formation of nitride phases. The addition of alloying elements in iron powders, such as titanium, chromium, vanadium, etc. which stabilize the ferrite, further stimulate nitrogen diffusion and the creation of nitride phases.

In the scientific literature, the influence of additional chemical thermal treatment on the elastic constants of sintered alloys has hardly been studied. In (Hirose, Oouchi, Fujiki, & Asami, 2006) article researchers studied the modulus of elasticity, shear modulus and Poisson's ratio of heat-treated samples made of diffusion alloyed Distaloy AE powder with addition of 0.8%C. By acoustic method it was found that the porosity, Young's modulus, and shear modulus changed from 29% to 27%, from 69.7GPa to 71.7GPa, and from 27.5 GPa to 28.2GPa, respectively, before and after the heat treatment.

Technical University of Varna Annual Journal
https://doi.org/10.29114/ajtuv.vol8.iss1.303
Vol. 8 Issue 1 (2024)
Published: 2024-06-28
ISSN 2603-316X (Online)

Authors (Gallo, Vitiello, & Prisco, 2003) investigated the influence of steam oxidation on the elastic constants. It was found that samples subjected to this type of treatment increase their modulus of elasticity, as the oxides created increase the density, and hence the studied modulus of elasticity.

In the field of application of chemical heat treatment of sintered alloys, the authors of the present study have extensive experience. This study aims to present experimental data concerning the elastic constants of iron-based alloys with the addition of 2% titanium, before and after application of low-temperature gas nitrocarburizing at different saturation times.

2 Materials and methodology

A raw base iron powder D.W.P200 was used. The powder is non alloyed, water atomized. The chemical composition is shown in table 1. The titanium powder was water atomized. Each powder was mixed to produce the material composition, which is 98wt%DWP200+2wt%Ti.

Table 1. Chemical composition of iron powder

Iron powder	**Chemical composition, %**						**Density /P=600MPa, 1% Zn stearate/, g/cm³**
D.W.P.200	C	Si	Mn	P	S	H_2-loss	
	≤0.01	≤0.05	≤0.20	≤0.020	≤0.015	≤0.20	≥6.95

Powder mixture (98%Fe+2%Ti) was uniaxially compacted at a pressure of 500MPa into 5x10x50mm compacts. Sintering was performed in industrial conditions in a tube furnace at T=1140°C, for 40 min, in a protective environment of 85%N_2:15%H_2 and furnace cooling.

The sintered specimens were nitrocarburized using low temperature gas nitrocarburizing (LTGNC) method performed at T=550°C (CARBONIT process), for 15 and 30 min., followed by furnace cooling. The process was carried out in a laboratory shaft furnace with a volume of 2 dm^3, in ammonia and carbon dioxide at an HN_3/CO_2=7.5/1 ratio.

The density of the samples, after sintering and LTGNC was determined by the geometric method, by measuring the dimensions of the samples and their weight (1). The microhardness was figured out using Vickers method. The sample surface was prepared using standard grinding and polishing procedure and etched in 3%NHO_3. The microstructure investigations were made with a light microscope.

$$\rho = \frac{m}{V}, \frac{g}{cm^3} \quad (1)$$

2.1. Measurement of dynamic Young's modulus and Shear modulus (G)

For the experimental determination of the elastic constants, a standard methodology based on the pulse resonance method according to the ASTM E1876-09 standard was used (Figure 1).

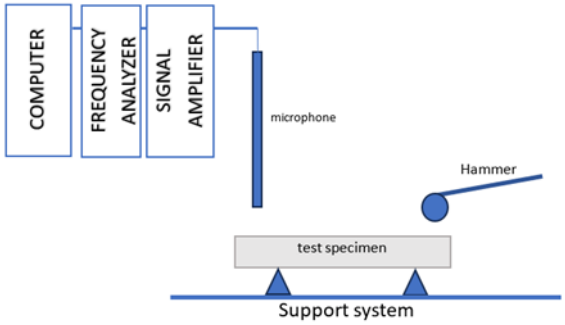

Fig. 1. Scheme of measurement of dynamic Young's modulus and shear modulus (G)

Technical University of Varna
Annual Journal
https://doi.org/10.29114/ajtuv.vol8.iss1.303
Vol. 8 Issue 1 (2024)
Published: 2024-06-28
ISSN 2603-316X (Online)

The specimen is placed on two supports spaced 0.224L from the ends and the fundamental mode frequency of the transverse bending vibrations is recorded. The eigenfrequency spectrum of the sample is excited by a light truncated impact with a hammer, which is a hardened steel sphere glued to a flexible rod. Figure 1. The response of the system is recorded contactless with a microphone connected to the sound card of the computer and with the help of specially developed LabView software it is converted into a frequency spectrum using the Fourier transform. Pressing the "START" button from the software turns on the microphone for 1s. At recording time, a hammer is struck. From the frequency spectrum, the frequency of the corresponding shape is read and the required module is calculated using (2). The same method was used to determine the shear modulus. The calculation was made by using formula (3).

$$\mathrm{E} = 0{,}9465.\frac{m.f_f^2}{b}.\frac{L^3}{t^3}.T_1 \quad (2)$$

$$G = \frac{4.L.m.f_t^2}{b.t}.R \quad (3)$$

where E– Young's modulus, (Pa); G– shear modulus, (Pa); m–specimen mass, (g); b, t, L -width, height and length of the specimen, (mm); f_f- frequency of fundamental bending mode shape, (Hz); ft- frequency of fundamental torsional mode shape, (Hz); T_1- correction coefficient depending on the L/t and the Poisson's coefficient ν. R-correction coefficient depending on the dimension ratios b/L and b/t. If L/t > 20 the influence of ν to coefficient T_1 can be ignored, otherwise ν should be known or the iterative procedure described below should be used. For R calculation it is recommended that the dimensions of the specimen be such that b/L < 0.3 and b/t < 10, otherwise the error may reach 1%.

3 Results and discussion

Table 2 shows the results of sintered density, Young's modulus and Shear modulus of sintered compacts. As it observed, by increasing density, Young's modulus is increased, as well the shear modulus.

According to the obtained dependences, it can be seen that at a sample density of 6.92 g/cm3, the modulus of elasticity is 160-164GPa, and as the density increases to 7-7.02 g/cm3, its values increase to 164-166GPa. The regression dependence was derived using a linear model. A similar relationship is also observed in the shear modulus data graph, where an increase with increasing sample density is recorded. Accordingly, the values for samples with low density are 64-65GPa, and for those with high - 66.5GPa.

Table 2. Results of sintered density, Young's modulus and Shear modulus of sintered compacts

Specimen	Density, g/cm^3	Young's modulus E, GPa	Shear modulus, GPa
1	6.92	160.207	64.211
2	7.00	164.869	65.667
3	7.00	164.237	65.341
4	7.01	166.366	66.09
5	6.94	163.599	65.268
6	7.00	166.785	66.233
7	6.92	163.808	65.054
8	6.96	166.833	66.296
9	6.92	163.196	64.998
10	7.00	166.397	66.249

Technical University of Varna
Annual Journal
https://doi.org/10.29114/ajtuv.vol8.iss1.303
Vol. 8 Issue 1 (2024)
Published: 2024-06-28
ISSN 2603-316X (Online)

Additional alloying of the iron powder with titanium, although in a small amount (2%), contributes to the activation of the sintering process, by creating a liquid phase, at the boundary of Fe and Ti particles. The liquid phase penetrates the pores located around the contact zone and fills them. Figure 2 shows the microstructure after sintering. The structure is ferrite, alloyed ferrite, TiFe-phases, undissolved Ti-particles, pores and oxides. The pores formed are of different shapes and sizes and are located both at the boundaries of the ferrite grains and in their volume. The structure is ferrite, alloyed ferrite, TiFe-phases, undissolved Ti-particles, pores and oxides. The pores formed are of different shapes and sizes and are located both at the boundaries of the ferrite grains and in their volume.

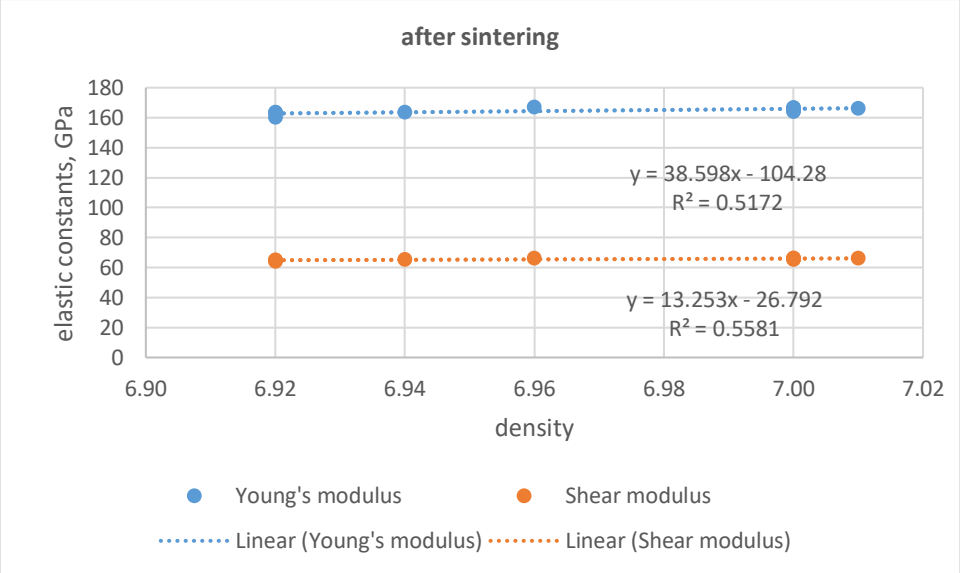

Fig. 2. Elastic constants after sintering

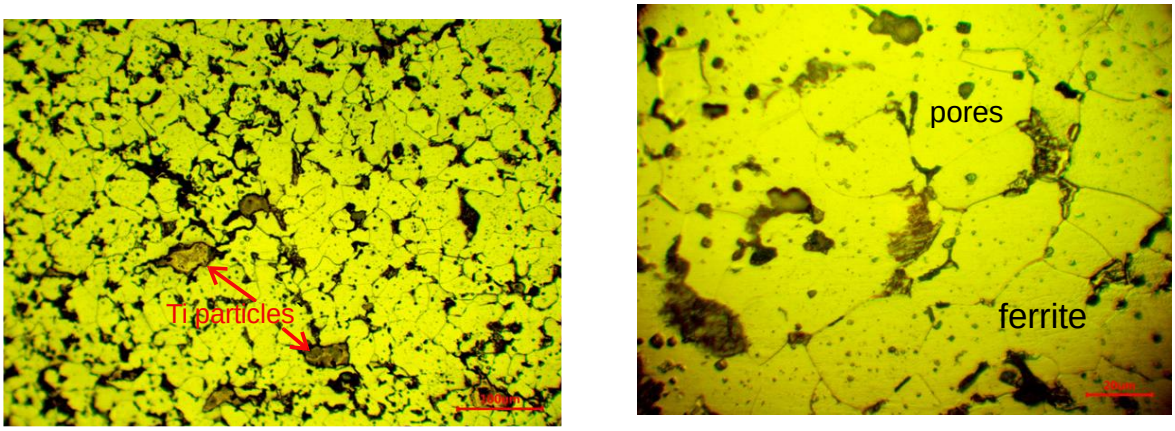

Fig. 3. Microstructure after sintering

After low-temperature gas nitrocarburizing regimes at different saturation times, it was found that the density of the samples increased relatively by about 1% compared to that after sintering and reached values around 7.01-7.03 g/cm^3. The higher density values were recorded for the samples saturated at the longer time.

The microstructures after chemical treatment, at different saturation times are shown in figures 2-5. White networks of ε+γ' phases are detected along ferrite grain boundaries throughout the sample volume. Needle-shaped γ' secondary separations are formed in the nitrogenous ferrite. A bonded layer of ε+γ' is formed on the surface of the samples. The thickness is about 3 – 4 μm (saturation time 15 min) (fig. 3).

Technical University of Varna
Annual Journal
https://doi.org/10.29114/ajtuv.vol8.iss1.303
Vol. 8 Issue 1 (2024)
Published: 2024-06-28
ISSN 2603-316X (Online)

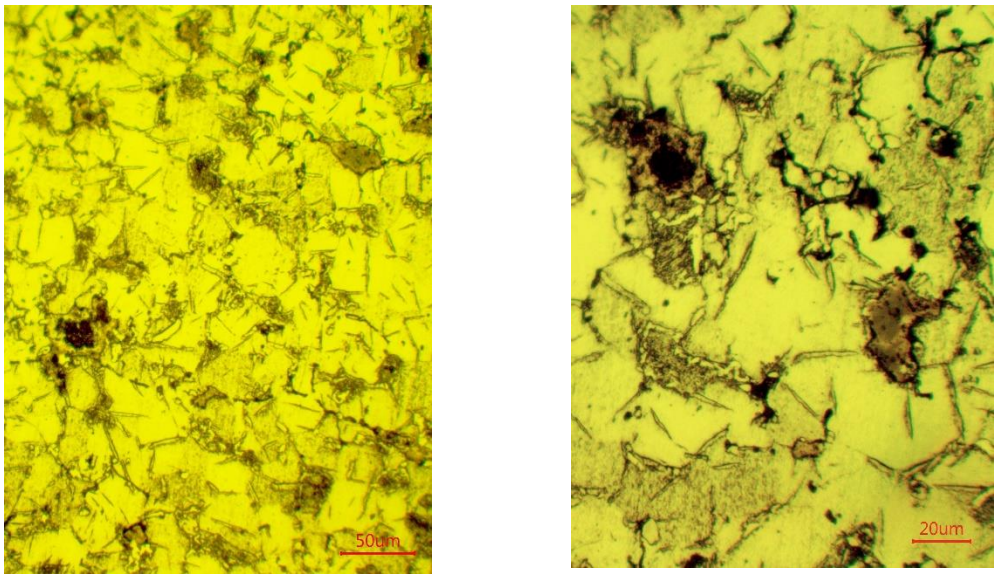

Fig. 4. Microstructure after LTGNC; saturation time 15 min; in the volume

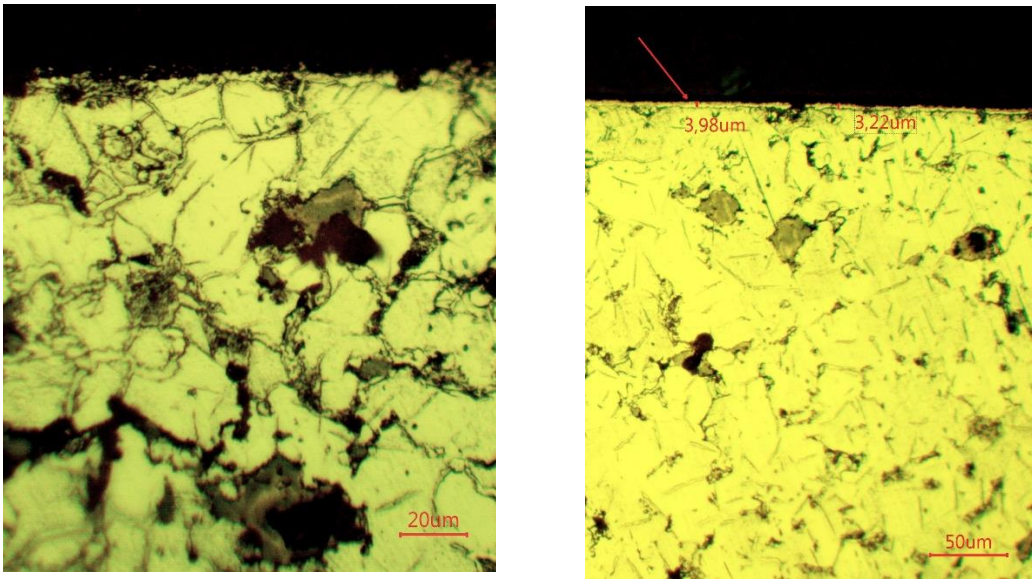

Fig. 5. Microstructure after LTGNC, 15 min saturation time, surface, etched

In some places the layer is discontinuous due to the presence of surface pores. Saturated ferrite grains are visible beneath the layer. This is probably due to the uneven density of the samples, with higher density on the densify side and lower on the opposite side. This contributes to the formation of the white bound zone in the higher density surface. Where the density is lower and the structure is defective, a prerequisite is created for more intense saturation and the formation of thicker nitride networks in the structure around the ferrite grains and intermetallic compounds.

Technical University of Varna
Annual Journal
https://doi.org/10.29114/ajtuv.vol8.iss1.303
Vol. 8 Issue 1 (2024)
Published: 2024-06-28
ISSN 2603-316X (Online)

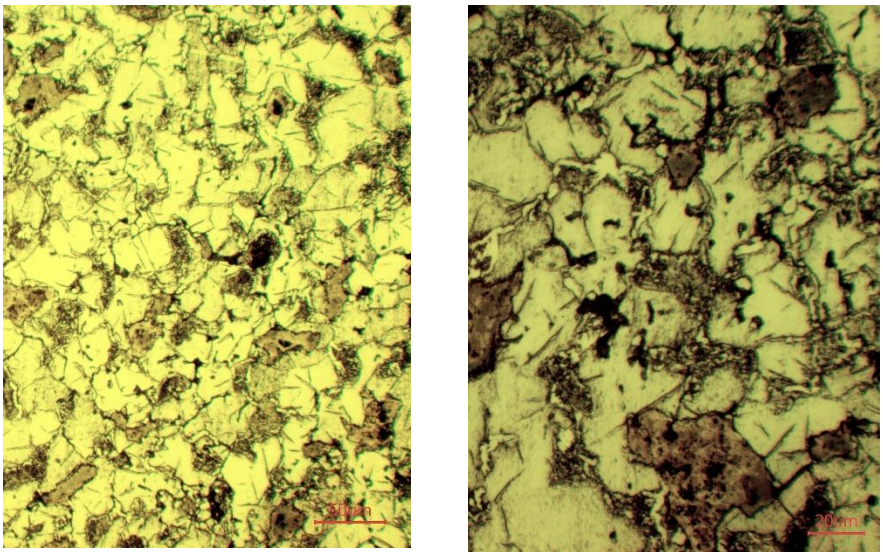

Fig. 6. Microstructure after LTGNC saturation time 30 min - volume

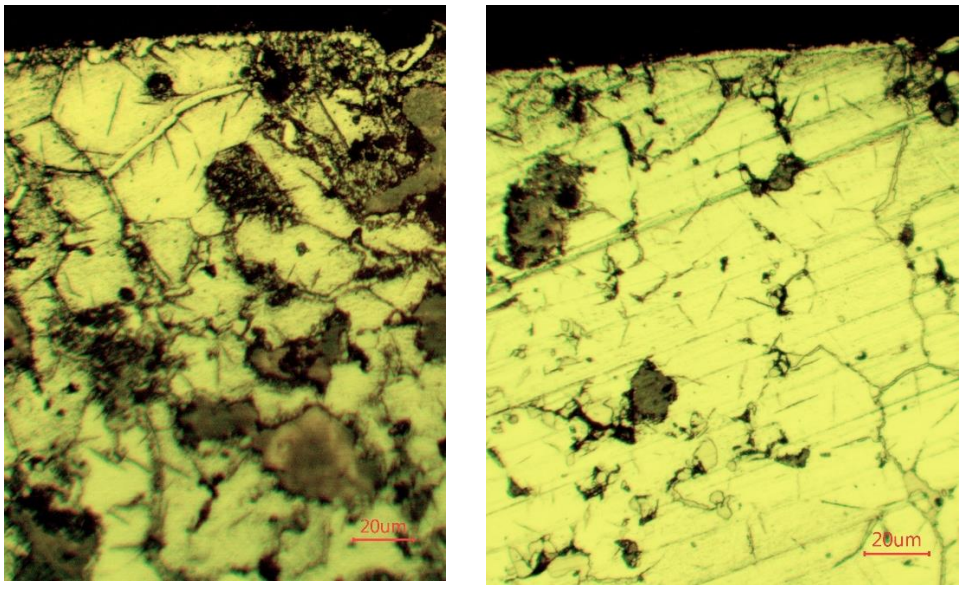

Fig. 7. Microstructure after LTGNC saturation time 30 min - surface

An increase in the microhardness of the samples was observed due to the formation of carbonitrided phases. The measured hardness at depth is in the range 195-120 HV0.05. (fig. 8). The measured hardness after sintering is about 80-100HV0.05.

Technical University of Varna
Annual Journal
https://doi.org/10.29114/ajtuv.vol8.iss1.303
Vol. 8 Issue 1 (2024)
Published: 2024-06-28
ISSN 2603-316X (Online)

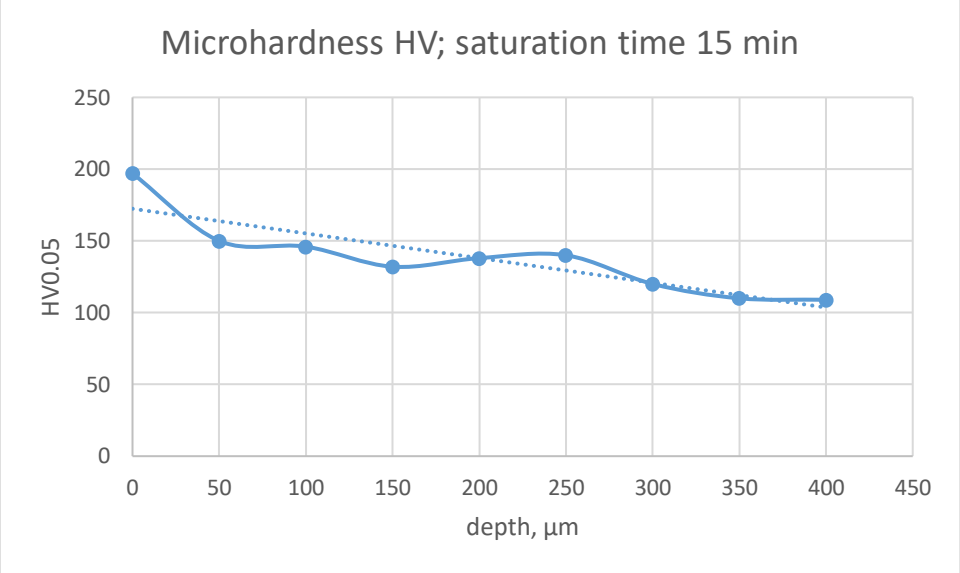

Fig. 8. Microhardness profile

The recorded increase in the density of the carbonitrided samples is a prerequisite to expect an increase in their elastic constants. After conducting the experiment and detailed data analysis, a slight increase in the value of elastic modulus was found in the range of 168-172GPa. With respect to the shear modulus, almost no difference in the values was observed after sintering and after chemical-heat treatment. Table 3 shows data from the measured moduli of elasticity for each sample that participated in the experiment.

Table 3. Density and elastic constants after LTGNC

Saturation time of nitrocarburizing	Density, g/cm^3	Young's modulus E, GPa	Shear modulus, GPa
30 min	7.01	167.027	66.318
	7.03	172.72	68.062
	7.01	169.372	66.743
	7.02	167.885	66.183
	7.03	168.756	66.859
15 min	7.02	171.399	67.483
	7.01	168.922	66.573
	7.01	167.61	66.498
	7.00	168.451	66.462
	7.02	172.383	68.144

4 Conclusion

Based on experimental studies the following conclusions can be drawn:

- Gas nitrocarburizing leads to an increase in the density of the samples
- Regarding the metallographic studies, it was found the presence of a formed surface layer of ε and γ' phases with a thickness of about 3-4µm, where the sample is without the presence of defect structure. The presence of nitride networks around the ferrite grains was found.

https://doi.org/10.29114/ajtuv.vol8.iss1.303
Vol. 8 Issue 1 (2024)
Published: 2024-06-28
ISSN 2603-316X (Online)

- An increase in elastic constants after chemical heat treatment regimes is reported.

Acknowledgement

The scientific research, the results of which are presented in this publication, have been carried out under a project SP8/2023 (НП8/2023) within the inherent research activities of TU-Varna funded by the state budget.

References

ASTM E1876-09 Standard Test Method for Dynamic Young's Modulus, Shear Modulus, and Poisson's Ratio by Impulse Excitation of Vibration.

Azabeh, M., Gierl, C., & Danninger, H. (2006). Elastic properties of Cr-Mo alloyed sinterd steels:A compariso of dynamic and static Young's moduli. *Powder Metallurgy Progress, Vol 6*, 1-10.

Chawla, N., & Deng, X. (2005). Microstructure an mechanical behavior of porous sintered steels. *Materials Science and Engineering*, 98-112. https://doi.org/10.1016/j.msea.2004.08.46

Dimitrov, D. M. (2013). Aplication of dynamic mtehods for determinnation of elastic constans of powder metallurgy materials. *NTD Days 2013*, 432-435.

Dimtrov, D. M., Mincheva, D., & Slavov, S. (2022). Influence of porosity to dynamic Young's modulus of sintered iron. Bayesian approach. *Materials Today Proceedings 59(21)*. https://doi.org/10.1016/j.matpr.2022.03.399

Galina, V., & Mannone, G. (1968). Effect of porosity and particle size on the mechanical strength of sintered iron. *Powder Metall.*, 77-82. https://doi.org/10.1179/pom.1968.11.21.006

Gallo, S. A., Vitiello, A., & Prisco, U. (2003). On control of Young's modulus of iron sintered part trough steam oxidation treatment. *Powder Meatllyrgy, 46, No1*. https://doi.org/10.1179/0033258903225010541

German, R. (1994). *Powder metallurgy.* New Jersey: Metal Powder Industries Federation.

Hirose, N., Oouchi, K., Fujiki, A., & Asami, J. (2006). Study of Elastic Moduli of Sintered Low Alloy Steels. *2006 POWDER METALLURGY World Congress* (pp. 387-388). Korean Powder Metallurgy Institute. https://doi.org/10.4028/0-87849-419-7.749.

Norimitsu, H., Asami, J., & Fujiki, A. (2004). Poison's ratio of sintered materials for structural machine parts. *Powder Metalurgy*, 515-525. https://doi.org/10.2497/jjspm.51.515.

Riera, M., Marba, I., & Prado, J. (2003). Elastic behavior under compressive stress states of sintered metallic parts. *Europian Congress and Exibition on Powder Metallurgy, EURO PM2003*, (pp. 447-452).

Ternero, F., Rosa, L. G., Urban, P., & Montes, J. (2021). Influence of the total porosity on the properties of sintered materials. *Metals*. https://doi.org/10.3390/met1150730